Engineering Science & Technology
http://ojs.wiserpub.com/index.php/EST/

UNIVERSAL WISER PUBLISHER

Research article

Influence of Triple Diffusive Convection in Peristaltic Flow of Jeffrey Nanofluid Through Non-Uniform Channel

S. K. Asha*, N. Kallolikar

Department of Mathematics, Karnatak University, Dharwad, Karnataka 580003, India
Email: as.kotnur2008@gmail.com

Received: 29 March 2022; **Revised:** 07 May 2022; **Accepted:** 17 May 2022

Abstract: In this investigation, we considered the effect of triple diffusive convection on peristaltic flow through a non-uniform Channel. We also considered the incompressible non-Newtonian Jeffrey nanofluid. On the assumption of a long wavelength and low Reynolds number, the governing equations were transformed into a non-dimensional form. The reduced non-dimensional highly nonlinear partial differential equations were solved using the Homotopy Perturbation Sumudu Transformation Method (HPSTM). The influence of different physical parameters on dimensionless velocity, pressure gradient, temperature, the concentration of salt 1 and salt 2, and volume fraction was graphically represented. The Dufour solutal Lewis number of salt 1 and salt 2 on the velocity profile increases. The Dufour solutal Lewis number and modified Dufour parameter of salt 1 rise on the nanoparticle volume fraction profile. It is found that the presence of the triple diffusing components with small diffusivity can change the convection in the system. The change in density in a triple diffusive is caused by the thermal and solutal diffusivities of two separate chemical species. So this study is applicable in engineering and scientific fields like geology, astrophysics, disposal of nuclear waste, Deoxyribonucleic Acid (DNA), and chemical engineering. This work is compared with the exact solution, and it is in good agreement with this method.

***Keywords*:** triple diffusion, peristaltic flow, Jeffrey nanofluid, non-uniform channel, HPSTM

Nomenclature

U', V'	velocity components
ρ_f	fluid density
g	gravitational acceleration
β_T	volumetric thermal expansion coefficient
β_{c_1}, β_{c_2}	volumetric solutal expansion coefficient of salt 1, 2
ρ_p	density of the particles
T	temperature of the fluid
C_1, C_2	solutal concentration of salt 1, 2
D_B	Brownian diffusion coefficient

DOI: https://doi.org/10.37256/est.3220221438

D_T	thermophoretic diffusion coefficient
D_{TC}, D_{CT}	Dufour and Soret type diffusivity
D_s	solutal diffusivity
Pr	Prandtl number
Gr_F	nanoparticle Grashof number
T_m	fluid mean temperature (K)
Gr_T	thermal Grashof number
N_{CT}	Soret parameter
Nb	Brownian motion parameter
Gr_{C_1}	solutal Grashof number of salt 1
Gr_{C_2}	solutal Grashof number of salt 2

1. Introduction

The study of the convection problem of multi-diffusivity (that is in the fluid more than one salt is present) is of great importance because of its usefulness in describing natural phenomena. The result of multi-diffusive convection was first studied by Griffiths [1]. Suppose the instability in a liquid is caused by three different diffusivities, then the mathematical and physical problems are termed three component convection or triple diffusive convection. Three constituents with different diffusivities result in triple diffusion. The use of triple diffusive convection can be seen in the modeling of a medical airing tool for the study of fatty acid anomalies, which includes various constituents such as saturated fat and triglycerides, molten alloy solidification, geothermally heated lakes, seawater, contaminant transport, underground water flow, and acid rain effects. Later, researchers [2]-[6] continue the study of triple diffusion in different flow geometric configurations.

Peristalsis pumping is a unique mechanism, and it is well known to physiologists as a natural mechanism for pumping materials. It is a form of fluid material transport induced by a progressive wave of area, either by contraction or expansion along the length of a distensible tube. It is known as peristaltic pumping. The peristaltic pump was first coined by Latham [7] and further research work on peristaltic flow was studied by Shapiro et al. [8], and Jaffrin et al. [9]. Further theoretic and experimental studies have been conducted on the various types of fluid flow in channels for peristalsis motion. The natural heat and mass transfer problem has become an interesting topic to study for researchers in industrial and biomedical areas. Some other studies are [10], [11]. The phenomenon of peristaltic transport in non-uniform ducts may be of considerable research interest. It is noted that many physiological problems are of the non-uniform cross-section. Gupta et al. [12] and Srivastava et al. [13] have considered peristaltic transport in non-uniform channels. It is seen in many physiological structures that the ducts are either in uniform or non-uniform cross-sections. It is well known that the human body is made up of several non-uniform ducts. Some other theoretical studies of peristalsis of biological fluids in non-uniform cross-sections are given in [14], [15].

Most of the physiological fluids behave as non-Newtonian fluids. The study of the Jeffrey fluid model is one of the most complex fluid models compared to other fluid models. Perhaps the first to bring this aspect into consideration were Raju and Devanathan [16]. The peristaltic flow of Jeffrey nanofluid is useful in physiology and industry with numerous applications and in mathematics due to its geometry and solutions to nonlinear equations. The Jeffrey fluid model, which acts as a Newtonian and non-Newtonian fluid depending on the nub region and perimetric region, was studied by Jyothi et al. [17] and Akbar et al. [18].

The prime objective of this study is to show the combined effect of heat and mass diffusion on a convective fluid mixture of two concentrations of salt 1 and salt 2, respectively. The investigation was carried out in a peristaltic flow of Jeffrey nanofluid. To the best of the authors' knowledge, no investigations have been reported on peristaltic pumping with a triple diffusivity fluid mixture of Jeffrey nanofluid in a non-uniform channel in the literature review. Especially, the investigation of triple diffusive fluid mixture is not given proper attention in the past. In the current world, such studies have substantial applications in improving scientific competence, developing new technologies, and contributing considerably to health. It also has uses in transportation, biomedical, and chemical engineering, as well as in industrial

processes. The mathematical formulation is made, and highly nonlinear partial differential equations are solved by HPSTM [19]-[21]. It's worth noting that the HPSTM finds the solution without the use of an initial guess and restrictive assumptions. It can also reduce the volume of computational work while maintaining high numerical accuracy, resulting in an improvement in the approach's performance. This approach has an obvious advantage over the decomposition method, in that it handles nonlinear problems without requiring Adomian's polynomials.

2. Mathematical formulation

Considering peristaltic flow in a two-dimensional non-uniform channel with the sinusoidal waves of small amplitudes, which proliferate the speed of the channel walls. c' is the constant speed of the channel (See Figure 1).

The geometric model of the channel is [11]

$$h'(\zeta,t) = a' + d\sin\left[\frac{2\pi}{\lambda}(\zeta' - c't')\right], \tag{1}$$

where the channel half width is $a' = a_0 + k\zeta$, c' is constant wave speed, λ is the wavelength, and t' and d are the time and the amplitude of the wave, respectively.

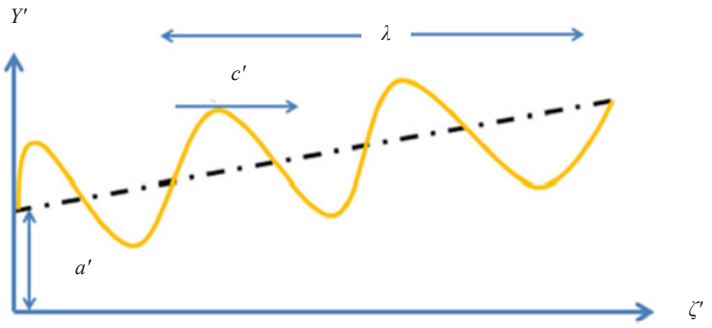

Figure 1. Geometry of the peristaltic transport through a non-uniform channel

U' and V' are the velocity components along the ζ' and y' directions, respectively, and the velocity field V is taken in the fixed frame as

$$V = [U'(\zeta', y', t'), V'(\zeta', y', t'), 0]. \tag{2}$$

The basic governing equations are [10], [11], [17]

$$\frac{\partial U'}{\partial \zeta'} + \frac{\partial V'}{\partial y'} = 0, \tag{3}$$

$$\rho_f\left(\frac{\partial U'}{\partial t'} + U'\frac{\partial U'}{\partial \zeta'} + V'\frac{\partial U'}{\partial y'}\right) = -\frac{\partial p'}{\partial \zeta'} + \frac{\partial S'_{xx}}{\partial \zeta'} + \frac{\partial S'_{xy}}{\partial y'} + \rho_f g(1 - F_0') \quad \{\beta_{C_1}(C_1' - C_0') + \beta_{C_2}(C_2' - C_0')$$

$$+\beta_T(T' - T_0')\} - g(\rho_p - \rho_{f_0})(F' - F_0'), \tag{4}$$

$$\rho_f\left(\frac{\partial V'}{\partial t'}+U'\frac{\partial V'}{\partial \zeta'}+V'\frac{\partial V'}{\partial y'}\right)=-\frac{\partial p'}{\partial \zeta'}+\frac{\partial S'_{xx}}{\partial \zeta'}+\frac{\partial S'_{xy}}{\partial y'}, \tag{5}$$

$$(\rho\overline{c})_f\left(\frac{\partial T'}{\partial t'}+U'\frac{\partial T'}{\partial \zeta'}+V'\frac{\partial T'}{\partial y'}\right)=k_T\left(\frac{\partial^2 T'}{\partial \zeta_2'}+\frac{\partial^2 T'}{\partial y_2'}\right)+\sigma D_{TC_1}\left(\frac{\partial^2 c_1}{\partial \zeta_2'}+\frac{\partial^2 c_1}{\partial y_2'}\right)+\sigma D_{TC_2}\left(\frac{\partial^2 c_2}{\partial \zeta_2'}+\frac{\partial^2 c_2}{\partial y_2'}\right)+$$

$$(\rho\overline{c})_p D_B\left(\frac{\partial F'}{\partial \zeta'}\frac{\partial T'}{\partial \zeta'}+\frac{\partial F'}{\partial y'}\frac{\partial T'}{\partial y'}\right)+(\rho\overline{c})_p\frac{D_T}{T_m}\left[\left(\frac{\partial T'}{\partial \zeta'}\right)^2+\left(\left(\frac{\partial T'}{\partial y'}\right)^2\right)\right]$$

$$+Br\left[\delta S_{xx}\frac{\partial u'}{\partial \zeta'}+S_{yy}\frac{\partial v'}{\partial y'}+S_{xy}\left(\delta\frac{\partial v'}{\partial \zeta'}+\frac{\partial u'}{\partial y'}\right)\right], \tag{6}$$

$$\frac{\partial c_1'}{\partial t'}+U'\frac{\partial c_1'}{\partial \zeta'}+V'\frac{\partial c_1'}{\partial y'}=D_{C_1T}\left(\frac{\partial^2 T'}{\partial \zeta_2'}+\frac{\partial^2 T'}{\partial y_2'}\right)+D_{sm_1}\left(\frac{\partial^2 c_1'}{\partial \zeta_2'}+\frac{\partial^2 c_1'}{\partial y_2'}\right), \tag{7}$$

$$\frac{\partial c_2'}{\partial t'}+U'\frac{\partial c_2'}{\partial \zeta'}+V'\frac{\partial c_2'}{\partial y'}=D_{C_2T}\left(\frac{\partial^2 T'}{\partial \zeta_2'}+\frac{\partial^2 T'}{\partial y_2'}\right)+D_{sm_2}\left(\frac{\partial^2 c_2'}{\partial \zeta_2'}+\frac{\partial^2 c_2'}{\partial y_2'}\right), \tag{8}$$

$$\frac{\partial F'}{\partial t'}+U'\frac{\partial F'}{\partial \zeta'}+V'\frac{\partial F'}{\partial y'}=D_B\left(\frac{\partial^2 F'}{\partial \zeta_2'}+\frac{\partial^2 F'}{\partial y_2'}\right)+\frac{D_T}{T_m}\left(\frac{\partial^2 T'}{\partial \zeta_2'}+\frac{\partial^2 T'}{\partial y_2'}\right), \tag{9}$$

where U' and V' are the velocity components along the ζ- and y-direction respectively, ρ_f is the fluid density, g is the gravitational acceleration, β_T is the volumetric thermal expansion coefficient, β_{c_1}, β_{c_1} and β_{c_2} are the volumetric solutal expansion coefficients of salt 1 and 2, respectively, ρ_P is the density of the particles, T is the temperature of the fluid, C_1 and C_2 are the solutal concentrations of salt 1 and 2, respectively, F is the nanoparticle concentration, D_B is the Brownian diffusion coefficient, D_T is the thermophoretic diffusion coefficient, D_{TC} and D_{CT} are the Dufour and Soret type diffusivity, and D_s is the solutal diffusivity.

The equation for incompressible non-Newtonian Jeffrey nanofluid is given as follows:

$$S=\frac{\mu}{\lambda_1+1}\left(\dot{\gamma}+\lambda_2\ddot{\gamma}\right), \tag{10}$$

where $\dot{\gamma}$ is the shear rate and dots denote the differentiation with respect to time, λ_1 is the ratio of relaxation to retardation time, μ is the dynamic viscosity, S is the stress tensor, and λ_2 is the retardation time.

The component form of equation (10) is defined as the following:

$$S_{\zeta\zeta}=\frac{2\mu}{1+\lambda_1}\left\{1+\lambda_2\left(\frac{\partial}{\partial t'}+V'\frac{\partial}{\partial Y'}+U'\frac{\partial}{\partial \zeta'}\right)\right\}\frac{\partial U'}{\partial \zeta'}, \tag{11}$$

$$S_{\zeta Y} = S_{Y\zeta} = \frac{\mu}{1+\lambda_1}\left\{1+\lambda_2\left(\frac{\partial}{\partial t'}+V'\frac{\partial}{\partial Y'}+U'\frac{\partial}{\partial \zeta'}\right)\right\}\left(\frac{\partial U'}{\partial Y'}+\frac{\partial V'}{\partial \zeta'}\right), \tag{12}$$

$$S_{YY} = \frac{2\mu}{1+\lambda_1}\left\{1+\lambda_2\left(\frac{\partial}{\partial t'}+V'\frac{\partial}{\partial Y'}+U'\frac{\partial}{\partial \zeta'}\right)\right\}\frac{\partial V'}{\partial Y'}, \tag{13}$$

The corresponding boundary conditions [11]

$$\psi' = 0,\ u' = \frac{\partial \psi'}{\partial y'} = 0,\ T' = T_0',\ C_1' = C_0',\ C_2' = C_0',\ F' = F_0', \text{ at } y' = 0, \tag{14}$$

$$\psi' = c,\ u' = \frac{\partial \psi'}{\partial y'} = -c,\ T' = T_1',\ C_1' = C_{1w}',\ C_2' = C_{2w}',\ F' = F_1', \text{ at } y' = h' = a' + d\sin\left[\frac{2\pi}{\lambda}(\zeta' - c't')\right], \tag{15}$$

Introducing non-dimensional variables

$$\psi = \frac{\psi'}{\overline{c}a_o}, \zeta = \frac{\zeta'}{\lambda}, y = \frac{y'}{a_o}, t = \frac{c't'}{\lambda}, v = \frac{v'}{c'}, \delta = \frac{a_o}{\lambda}, p = \frac{p'{a_o}^2}{\mu\overline{c}\lambda}, h = \frac{h'}{a_o},$$

$$u = \frac{u'}{\overline{c}}, \alpha = \frac{k_T}{(\rho\overline{c})_f}, b = \frac{d}{a_o}, \theta = \frac{T'-T_0'}{T_1'-T_0'}, \chi_1 = \frac{C_1'-C_{10}'}{C_{1w}'-C_{10}'}, \chi_2 = \frac{C_2'-C_{20}'}{C_{2w}'-C_{20}'},$$

$$\gamma = \frac{F'-F_0'}{F_1'-F_0'}, Nt = \frac{(\rho\overline{c})_p D_T(T_1'-T_0')}{(\rho\overline{c})_f \mu T_m}, Nd_1 = \frac{\sigma D_{TC_1}(C_1-C_{10})}{K_T(T_1'-T_0')}, f^* = \frac{q}{\overline{c}a_o},$$

$$Nd_2 = \frac{\sigma D_{TC_2}(C_2-C_{20})}{K_T(T_1'-T_0')}, Gr_t = \frac{\rho_f g{a_o}^2(T_1'-T_0')\beta_T(1-F_0)}{\overline{c}\mu}, \Pr = \frac{(\rho\overline{c})_f \mu}{K_T},$$

$$Gr_{c_1} = \frac{\rho_f g{a_o}^2(C_1'-C_{10})\beta c_1(1-F_0)}{\overline{c}\mu}, Gr_{c_2} = \frac{\rho_f g{a_o}^2(C_2'-C_{20})\beta c_2(1-F_0)}{\overline{c}\mu},$$

$$N_{TC} = \frac{D_{CT}(T_1'-T_0')}{D_s(F_1'-F_0')}, Gr_F = \frac{(\rho_p-\rho_{f_0})g{a_o}^2(F_1'-F_0')}{\overline{c}\mu}, Ld_2 = \frac{D_{C_2T}(T_1'-T_0')}{D_{Sm_2}(C_2'-C_{20})},$$

$$Nb = \frac{(\rho\overline{c})_p D_B(F_1'-F_0')}{(\rho\overline{c})_f \mu}, Ld_1 = \frac{D_{C_1T}(T_1'-T_0')}{D_{Sm_1}(C_1'-C_{10})}, \tag{16}$$

Here δ is the wave number, θ is temperature, and γ is volume fraction, which are all in dimensionless form, and the stream function is taken as $v = -\delta\frac{\partial\psi}{\partial\zeta}$ and $u = \frac{\partial\psi}{\partial y}$.

The non-dimensional governing equations are

$$\frac{\partial p}{\partial \zeta} = \frac{\partial}{\partial y}\left(\frac{1}{1+\lambda_1}\frac{\partial^2 u}{\partial y^2}\right) + Gr_T\theta + Gr_{C_1}\chi_1 + Gr_{C_2}\chi_2 - Gr_F\gamma, \tag{17}$$

$$\frac{\partial P}{\partial y} = 0, \tag{18}$$

Using equations (17) and (18), we get the velocity equation as follows

$$\frac{1}{1+\lambda_1}\frac{\partial^3 \psi}{\partial y^3} + Gr_T\frac{\partial \theta}{\partial y} + Gr_{C_1}\frac{\partial \chi_1}{\partial y} + Gr_{C_2}\frac{\partial \chi_2}{\partial y} - Gr_F\frac{\partial \gamma}{\partial y} = 0, \tag{19}$$

$$\frac{\partial^2 \theta}{\partial y^2} + Nb\,\mathrm{Pr}\frac{\partial \theta}{\partial y}\frac{\partial \gamma}{\partial y} + Nd_1\frac{\partial^2 \chi_1}{\partial y^2} + Nd_2\frac{\partial^2 \chi_2}{\partial y^2} + Nt\,\mathrm{Pr}\left(\frac{\partial \theta}{\partial y}\right)^2 = 0, \tag{20}$$

$$\frac{\partial^2 \chi_1}{\partial y^2} + Ld_1\frac{\partial^2 \theta}{\partial y^2} = 0, \tag{21}$$

$$\frac{\partial^2 \chi_2}{\partial y^2} + Ld_2\frac{\partial^2 \theta}{\partial y^2} = 0, \tag{22}$$

$$\frac{\partial^2 \gamma}{\partial y^2} + \frac{Nt}{Nb}\frac{\partial^2 \theta}{\partial y^2} = 0. \tag{23}$$

A dimensionless boundary condition is as follows

$$\psi = 0,\ \frac{\partial \psi}{\partial y} = 0,\ \theta = 0,\ \chi_1 = 0,\ \chi_2 = 0,\ \gamma = 0, \text{ at } y = 0, \tag{24}$$

$$\psi = f^*,\ \frac{\partial \psi}{\partial y} = -1,\ \theta = 1,\ \chi_1 = 1,\ \chi_2 = 1,\ \gamma = 1, \text{ at } y = h = 1 + \frac{\lambda k_0 \zeta}{a_0} + b\sin\left[2\pi\left(x - t\right)\right]. \tag{25}$$

Where f^* is the wave frame and it is associated with the time-mean flow rate Θ which is dimensionless in the laboratory frame, as mentioned below:

$$\Theta = f^* + 1,\ f^* = \int_0^h \frac{\partial \psi}{\partial y}\,dy, \tag{26}$$

where $\Theta = \frac{Q}{sa_0}$ and $f^* = \frac{q}{sa_0}$ are the time-mean flow rate in fixed and wave frames, respectively. The non-dimensional governing equations (17) to (23) using boundary condition (24) are solved using HPSTM.

3. Methodology

The partial differential equations (17) to (23) are solved by HPSTM, which is an analytical technique. It is used to calculate a nonlinear problem that comprises large and small physical parameters (convergent series is obtained after solving).

To obtain an approximate analytical solution, we apply the HPSTM to the governing equations. We get the following equation after applying the Sumudu and inverse Sumudu transforms into the governing equations on both sides [19].

$$u(y)=\left(1+\lambda_1\right)A\frac{y^2}{2}-s^{-1}\left[\left(1+\lambda_1\right)v^3 s\left[Gr_T\frac{\partial\theta}{\partial \mathrm{y}}-Gr_{C_1}\frac{\partial\chi_1}{\partial \mathrm{y}}+Gr_{C_2}\frac{\partial\chi_2}{\partial \mathrm{y}}+Gr_F\frac{\partial\gamma}{\partial \mathrm{y}}\right]\right], \tag{27}$$

$$\theta(y)=Ay-s^{-1}\left[u^2 s\left[Nb\,\mathrm{Pr}\frac{\partial\theta}{\partial y}\frac{\partial\gamma}{\partial y}+Nd_1\frac{\partial^2\chi_1}{\partial y^2}+Nd_2\frac{\partial^2\chi_2}{\partial y^2}+Nt\,\mathrm{Pr}\left(\frac{\partial\theta}{\partial y}\right)^2\right]\right], \tag{28}$$

$$\chi_1(y)=Ay-s^{-1}\left[u^2 s\left[Ld_1\frac{\partial^2\theta}{\partial y^2}\right]\right], \tag{29}$$

$$\chi_2(y)=Ay-s^{-1}\left[u^2 s\left[Ld_2\frac{\partial^2\theta}{\partial y^2}\right]\right], \tag{30}$$

$$\gamma(y)=Ay-s^{-1}\left[u^2 s\left[\frac{Nt}{Nb}\frac{\partial^2\theta}{\partial y^2}\right]\right]. \tag{31}$$

Now applying HPM, and coefficients of like powers of P were compared using He's polynomial, which is given below

$$H_m(U_0,U_1,U_{2,\ldots\ldots}U_m)=\frac{1}{m!}\frac{\partial^m}{\partial p^m}\left[N\left(\sum_{i=0}^{\infty}p^i U_i\right)\right]_{p=0} \tag{32}$$

The required series solution is as follows,

$$u=\frac{1+\lambda_1}{2}Ay^2-\left(1+\lambda_1\right)\left(\left(Grc_1A\frac{y^3}{6}+Grc_2A\frac{y^3}{6}\right)+Gr_TA\frac{y^3}{6}-Gr_FA\frac{y^3}{6}\right)$$

$$-\left(1+\lambda_1\right)\left(Gr_TA\frac{y^4}{24}Nb\,\mathrm{Pr}-Gr_TA\frac{y^4}{24}Nt\,\mathrm{Pr}\right)+\ldots\ldots\ldots\ldots, \tag{33}$$

$$\theta = Ay - Nb\,\mathrm{Pr}\,A^2\frac{y^2}{2} - Nt\,\mathrm{Pr}\,A^2\frac{y^2}{2} + Nb^2\,\mathrm{Pr}^2\,A^3\frac{y^3}{6} + NbNt\,\mathrm{Pr}^2\,A^3\frac{y^3}{6}$$

$$-Nt\,\mathrm{Pr}\left(-Nb\,\mathrm{Pr}\,A^2 - Nt\,\mathrm{Pr}\,A^2\right)^2\frac{y^4}{48} + \ldots\ldots\ldots, \tag{34}$$

$$\chi_1 = Ay + Nb\,\mathrm{Pr}\,Ld_1A^2\frac{y^3}{6} + Nt\,\mathrm{Pr}\,Ld_1A^2\frac{y^3}{6} - Nb^2\,\mathrm{Pr}^2\,Ld_1A^3\frac{y^3}{6} - NtNb\,\mathrm{Pr}^2\,Ld_1A^3\frac{y^3}{6}$$

$$+Nt\,\mathrm{Pr}\,Ld_1\left(-Nb\,\mathrm{Pr}\,A^2 - Nt\,\mathrm{Pr}\,A^2\right)^2\frac{y^4}{192} + \ldots\ldots\ldots, \tag{35}$$

$$\chi_2 = Ay + Nb\,\mathrm{Pr}\,Ld_2A^2\frac{y^3}{6} + Nt\,\mathrm{Pr}\,Ld_2A^2\frac{y^3}{6} - Nb^2\,\mathrm{Pr}^2\,Ld_2A^3\frac{y^3}{6} - NtNb\,\mathrm{Pr}^2\,Ld_2A^3\frac{y^3}{6}$$

$$+Nt\,\mathrm{Pr}\,Ld_2\left(-Nb\,\mathrm{Pr}\,A^2 - Nt\,\mathrm{Pr}\,A^2\right)^2\frac{y^4}{192} + \ldots\ldots\ldots, \tag{36}$$

$$\gamma = Ay + Nt\,\mathrm{Pr}\,A^2\frac{y^2}{2} + \frac{Nt^2\,\mathrm{Pr}}{Nb}A^2\frac{y^2}{2} - NbNt\,\mathrm{Pr}^2\,A^2\frac{y^3}{6} - Nt^2\,\mathrm{Pr}^2\,A^3\frac{y^3}{6}$$

$$+\frac{Nt^2\,\mathrm{Pr}}{Nb}\left(-Nb\,\mathrm{Pr}\,A^2 - Nt\,\mathrm{Pr}\,A^2\right)^2\frac{y^4}{192} + \ldots\ldots\ldots\ldots\ldots \tag{37}$$

The volume flow rate is given by

$$Q = \int_0^h u dy. \tag{38}$$

Integrating equation (34) and after manipulating, we obtain a pressure gradient.

4. Results and discussion

Using HPSTM, we have solved the nonlinear partial differential equations. We have used the symbolic software Mathematica in this work. The velocity, pressure gradient, temperature, volume fraction of nanoparticles, and solutal (species) concentration profiles of salt 1 and salt 2 are solved through the codes of the software Mathematica and graphic outcomes are plotted in Origin Software. The obtained results of volume fraction and temperature are compared with the exact solution shown in Tables 1 and 2, respectively. It is in good agreement with the present method.

Table 1. A comparison of the numerical values of the volume fraction profile by the exact solution with HPSTM. For the values of $Nb = 0.01$, $Nt = 0.5$, $Ld_1 = 0.0$, $Ld_2 = 0.0$, $Nd_1 = 0.0$, $Nd_2 = 0.0$, Pr = 1.

y	Exact solution	Present work
0.0	0.0	0.0
0.2	0.199968	0.19996
0.4	0.399936	0.39993
0.6	0.599904	0.5999
0.8	0.799871	0.79987
1.0	0.999836	1.0

Table 2. A comparison of the numerical values of the temperature profile by the exact solution with HPSTM. For the values of $Nb = 0.1$, $Nt = 0.5$, $Ld_1 = 0.0$, $Ld_2 = 0.0$, $Nd_1 = 0.0$, $Nd_2 = 0.0$, Pr = 1.

y	Exact solution	Present work
0.0	0.0	0.0
0.2	0.333821	0.333821
0.4	0.592298	0.592294
0.6	0.784385	0.784381
0.8	0.917996	0.917994
1.0	1.0	1.0

4.1 *Velocity distribution*

From Figures 2, 3, 4, and 5, we can observe the effects of solutal Grashof number Gr_{C_1}, Jeffrey fluid parameter λ_1, Dufour solutal Lewis number of salt 1 Ld_1 and Dufour solutal Lewis number of salt 2 Ld_2 respectively on velocity profile. It is observed in Figure 2 that as the solute Grashof number Gr_{C_1} increases, the velocity profile also increases. This is because, Gr_{C_1} is inversely proportion to the viscosity of the fluid, which increases the velocity of the fluid. The same result can be observed in Jeffrey fluid parameter λ_1, which is shown in Figure 3. From Figures 4 and 5, we can observe that u increases with increasing values of Ld_1 and Ld_2. This is because Ld_1 and Ld_2 specify the impact of thermal gradient on concentration, the concentration gradient accelerates the flow, and thus the velocity profile increases.

4.2 *Pressure gradient*

The effects of solutal Grashof number Gr_{C_1}, and Dufour solutal Lewis number of salt 1 Ld_1 on pressure gradient are represented in Figures 6 and 7. It is observed in Figure 6 that as solutal Grashof number Gr_{C_1} increases, pressure gradient increases. This is because, as the concentration of nanoparticles in the fluid increases, pressure gradient increases. In Figure 7, we have observed that as Dufour solutal Lewis number of salt 1 Ld_1 rises, pressure gradient also rises.

4.3 *Temperature profile*

Through Figures 8-11, we can observe the effect of Nb, Nt, Nd_1, and Ld_1 respectively on θ. We can see that there is an enhancement in θ for different values of Nb, and Nt, which is shown in Figures 8 and 9, respectively. More heat is produced due to the arbitrary movement of fluid particles as the Brownian motion parameter increases, which is shown in Figure 8. By enhancing Nt, the θ rises as the fluid particles migrate from cold to a hot surface, shown in Figure 9. From Figure 10, we can observe that θ rises when the modified Dufour parameter of salt 1 Nd_1 rises. As the value of Nd_1 grows larger, the temperature rises due to the increased thermal diffusivity. When the thermal diffusivity increases, the thermal conductivity increases, the molecular vibration increases, and therefore, the temperature increases. From Figure 11, we can see that the Dufour solutal Lewis number of salt 1 Ld_1 increases, respectively. This is due to the fact that Ld_1 specifies the impact of thermal gradient on concentration, and concentration gradient stimulates the flow along with the enhancement of thermal energy.

4.4 *The concentration of salt 1*

From Figures 12 and 13, we can observe the effects of Nb and Ld_1 on the concentration of salt 1 respectively for different values. The concentration of salt 1 increases with increasing values of Nb, which is shown in Figure 12. That is, with an increment of Nb, a temperature gradient force is produced, which boosts the flow of concentration. In Figure 13, we can observe that a significant increase in solutal concentration profile χ_1 can be seen for increasing values of Ld_1 because of greater mass diffusivity. Higher mass diffusivity indicates a higher chance of molecular collision due to a major difference in solutal concentration. The difference in solutal concentration of molecules rises as the concentration gradient rises. Increased mass diffusivity enhances the solutal concentration gradient, resulting in increased solutal concentration and thickening of the associated boundary layer, as shown.

4.5 *The concentration of salt 2*

From Figures 14 and 15, we can observe the effects of Nb, and Ld_2 on concentration of salt 2 respectively for different values. The concentration of salt 2 increases with increasing values of the Brownian motion parameter Nb, which is shown in Figure 14. That is, with an increment of the Nb, a temperature gradient force is produced, which boosts the flow of concentration. In Figure 15, we can observe that a significant increase in solutal concentration profile χ_2 can be seen for increasing values of Dufour solutal Lewis number of salt 2 Ld_2 because of greater mass diffusivity. Higher mass diffusivity indicates a higher chance of molecular collision due to a major difference in solutal concentration. The difference in solutal concentration of molecules rises as the concentration gradient rises. Increased mass diffusivity enhances the solutal concentration gradient, resulting in increased solutal concentration and thickening of the associated boundary layer, as shown.

4.6 *Volume fraction*

Figures 16 and 17 represent the effect of the Dufour solutal Lewis number of salt 1 Ld_1 and modified Dufour parameter of salt 1 Nd_1 on volume fraction. We can observe that as Ld_1 increases, volume fraction profile also increases. Nanoparticle concentration and Ld_1 are inversely proportional to the difference in the density of the fluid at the channel. As a result, the higher the Ld_1, the higher the nanoparticle concentration will be. These measurements demonstrate a considerable rise in the nanoparticle's volume fraction profile as a result of higher mass diffusivity. Due to a considerable difference in the density of the particles, the increased mass diffusivity indicates a greater chance of molecular collision. So, nanoparticle volume fraction profile increases with increases of Ld_1, as shown in Figure 16, and Figure 17 depicts the effect of Nd_1 on volume fraction profile. That is, as Nd_1 increases, volume fraction profile also increases.

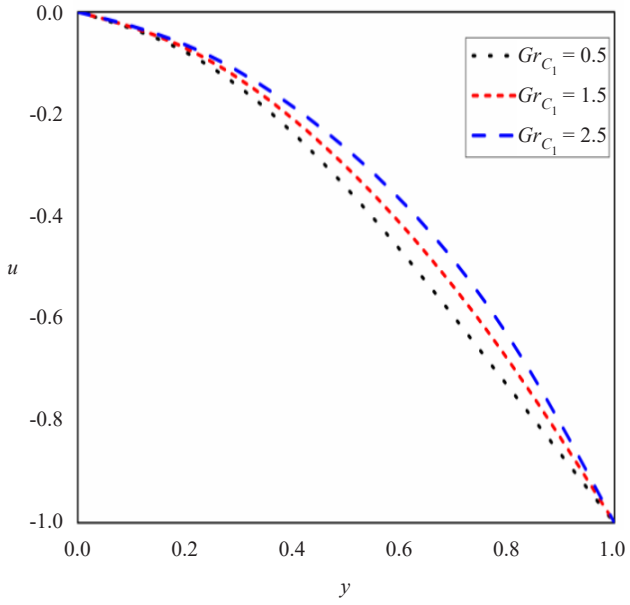

Figure 2. Variation of Gr_{C_1} on u
$Nb = 0.8$, $Nt = 0.8$, $Ld_1 = 0.8$, $Ld_2 = 0.8$, $Nd_1 = 0.8$, $Nd_2 = 0.8$, $Gr_{C_2} = 0.8$, $Gr_T = 0.8$, $Gr_F = 0.8$, $\Pr = 2\lambda_1 = 1$

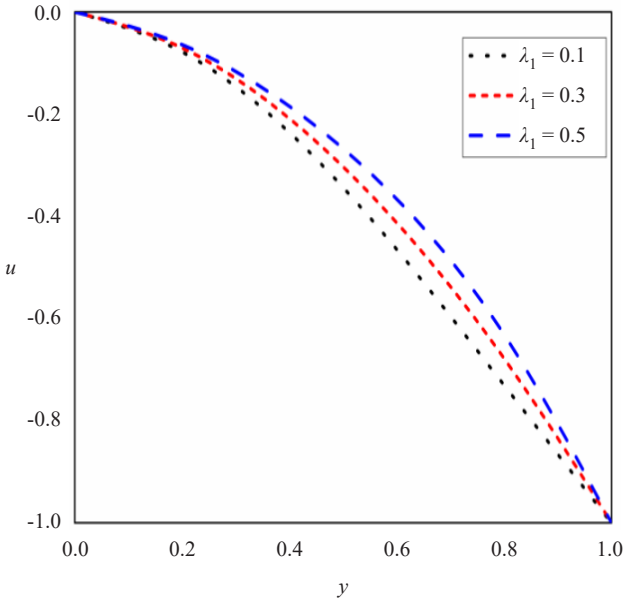

Figure 3. Variation of λ_1 on u
$Nb = 0.8$, $Nt = 0.8$, $Ld_1 = 0.8$, $Ld_2 = 0.8$, $Nd_1 = 0.8$, $Nd_2 = 0.8$, $Gr_{C_1} = 0.8$, $Gr_{C_2} = 0.8$, $Gr_T = 0.8$, $Gr_F = 0.8$, $\Pr = 2\lambda_1 = 1$

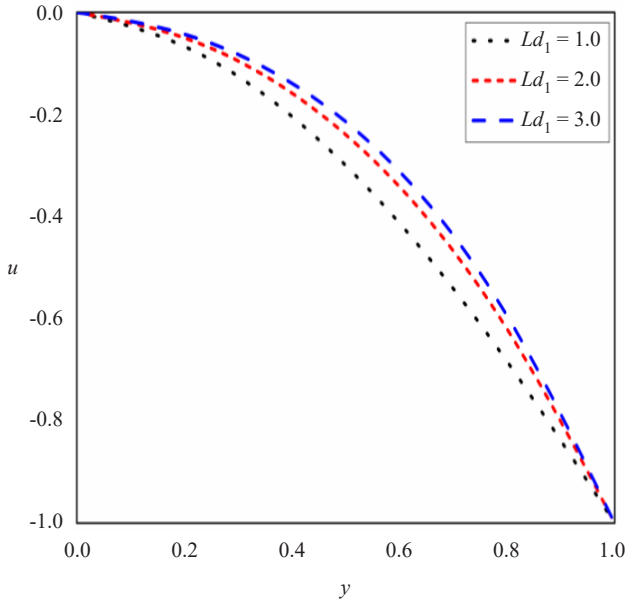

Figure 4. Variation of Ld_1 on u
$Nb = 0.8$, $Nt = 0.8$, $Ld_1 = 0.8$, $Ld_2 = 0.8$, $Nd_1 = 0.8$, $Nd_2 = 0.8$, $Gr_{C_1} = 0.8$, $Gr_{C_2} = 0.8$, $Gr_T = 0.8$, $Gr_F = 0.8$, $\Pr = 2\lambda_1 = 1$

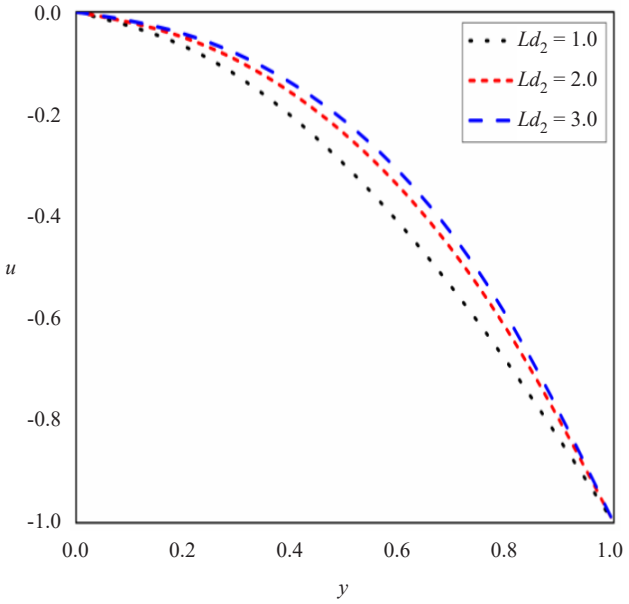

Figure 5. Variation of Ld_2 on u
$Nb = 0.8$, $Nt = 0.8$, $Ld_1 = 0.8$, $Ld_2 = 0.8$, $Nd_1 = 0.8$, $Nd_2 = 0.8$, $Gr_{C_1} = 0.8$, $Gr_{C_2} = 0.8$, $Gr_T = 0.8$, $Gr_F = 0.8$, $\Pr = 2\lambda_1 = 1$

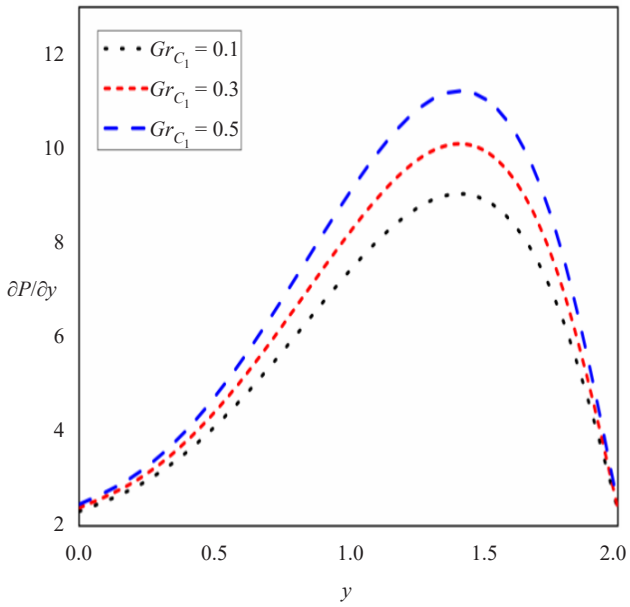

Figure 6. Variation of Gr_{C_1} on $\frac{\partial P}{\partial y}$
$Nb = 0.3$, $Nt = 0.3$, $Ld_1 = 0.3$, $Ld_2 = 0.3$, $Gr_{C_2} = 0.3$, $Gr_T = 0.3$, Pr = 5

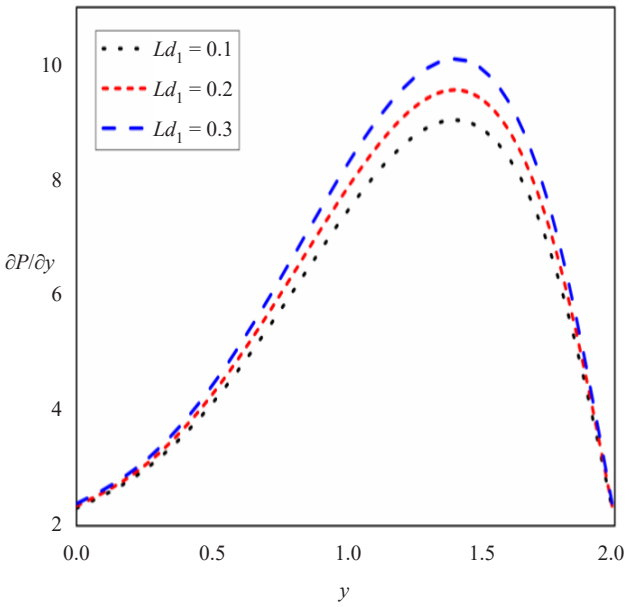

Figure 7. Variation of Ld_1 on $\frac{\partial P}{\partial y}$
$Nb = 0.3$, $Nt = 0.3$, $Ld_2 = 0.3$, $Gr_{C_1} = 0.3$, $Gr_{C_2} = 0.3$, $Gr_T = 0.3$, Pr = 5

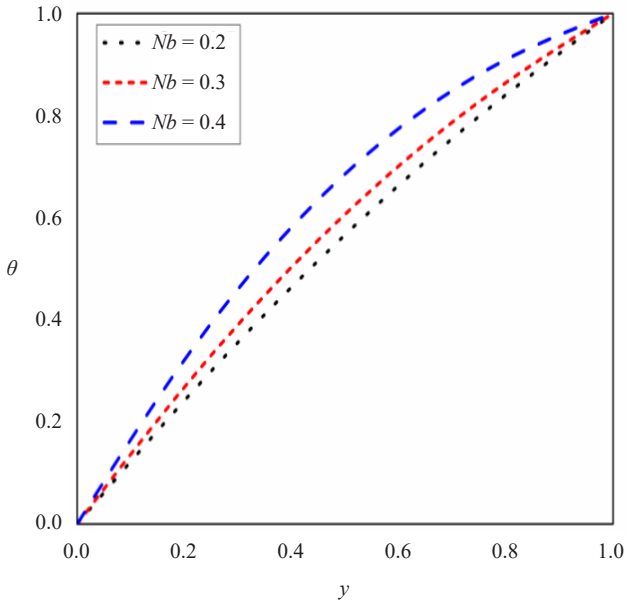

Figure 8. Variation of Nb on θ
$Nb = 0.1$, $Nt = 0.1$, $Ld_1 = 0.5$, $Ld_2 = 0.5$, $Nd_2 = 0.5$, Pr = 1

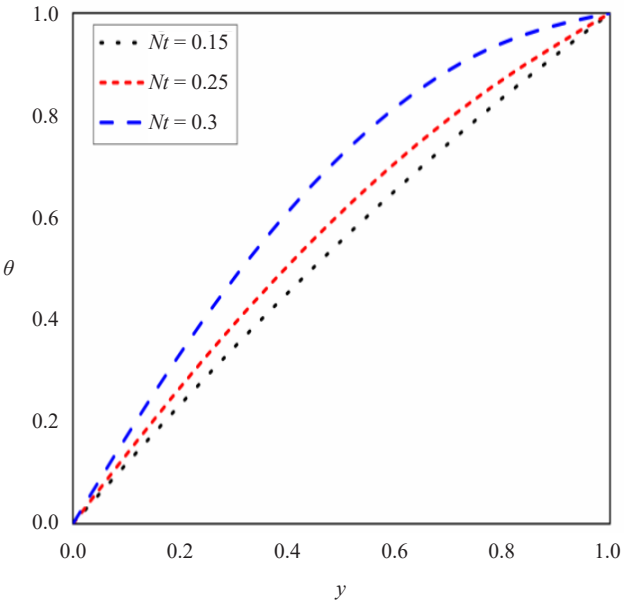

Figure 9. Variation of Nt on θ
$Nb = 0.1$, $Ld_1 = 0.5$, $Ld_2 = 0.5$, $Nd_1 = 0.5$, $Nd_2 = 0.5$, Pr = 1

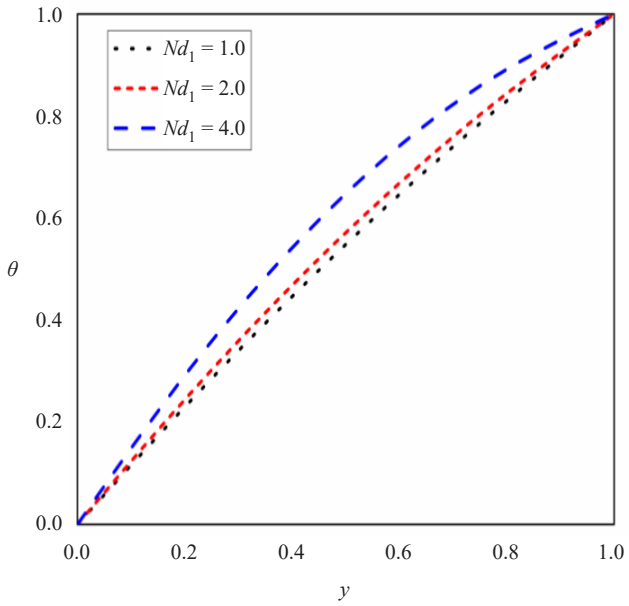

Figure 10. Variation of Nd_1 on θ
$Nb = 0.1$, $Nt = 0.1$, $Ld_1 = 0.5$, $Ld_2 = 0.5$, $Nd_2 = 0.5$, Pr = 1

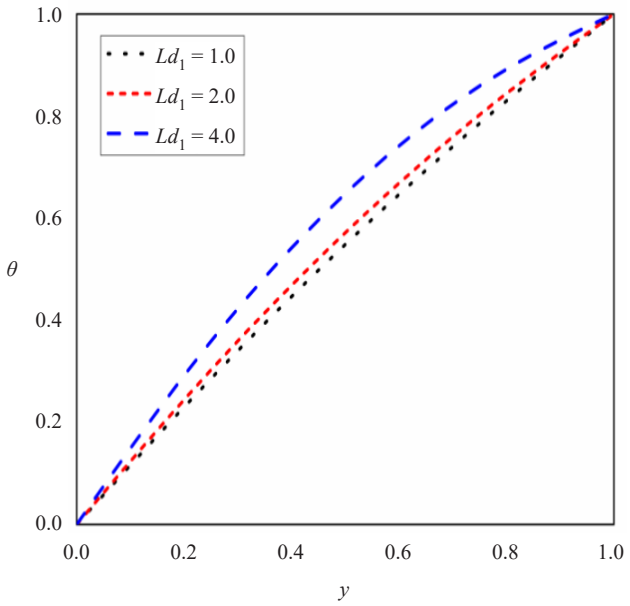

Figure 11. Variation of Ld_1 on θ
$Nb = 0.1$, $Nt = 0.1$, $Ld_2 = 0.5$, $Nd_1 = 0.5$, $Nd_2 = 0.5$, Pr = 1

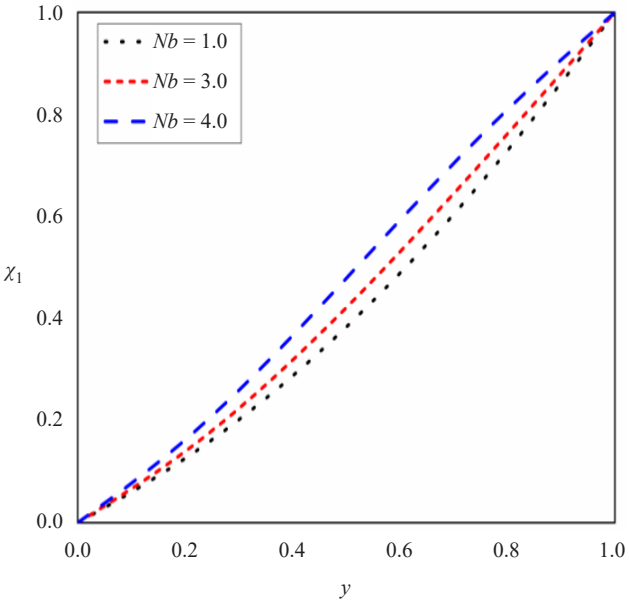

Figure 12. Variation of Nb for χ_1
$Nt = 4.0$, $Ld_1 = 1$, Pr = 1

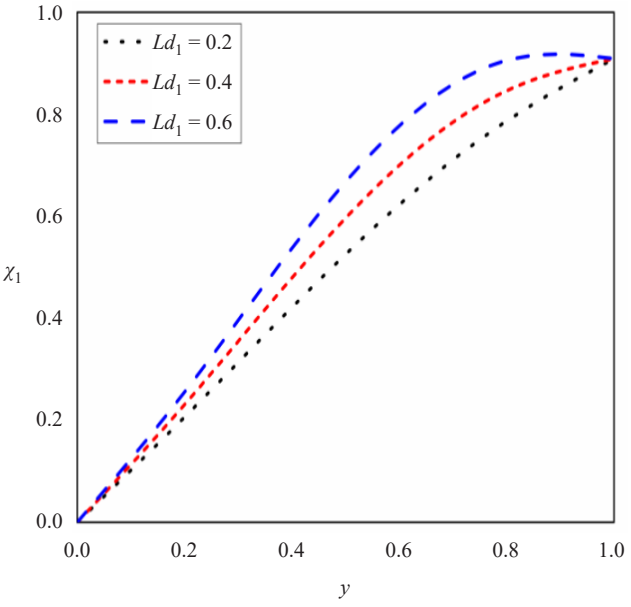

Figure 13. Variation of Ld_1 for χ_1
$Nb = 4.0$, $Nt = 1$, Pr = 1

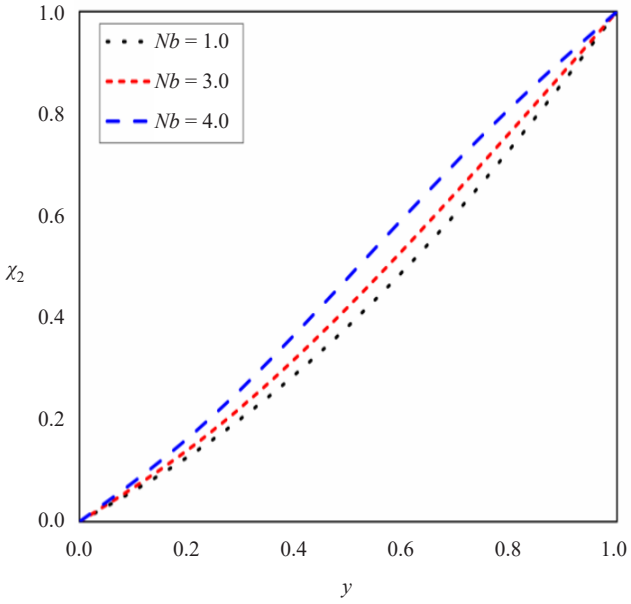

Figure 14. Variation of Nb for χ_2
$Nt = 4.0$, $Ld_1 = 1$, $Ld_2 = 1$, Pr = 1

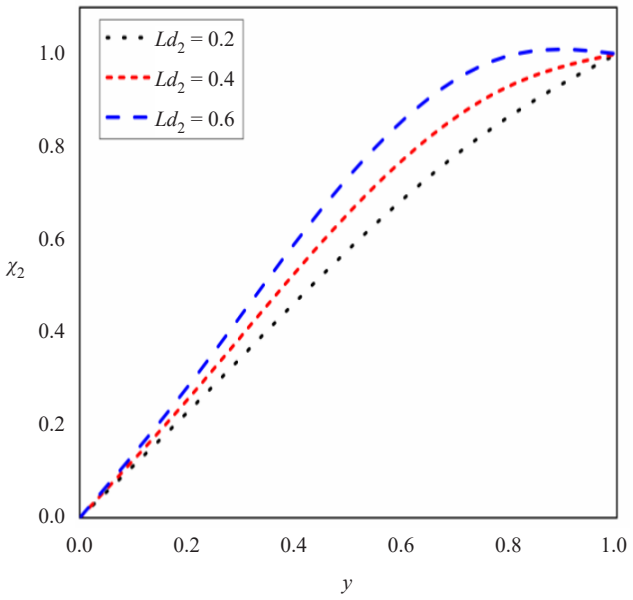

Figure 15. Variation of Ld_2 for χ_2
$Nb = 4.0$, $Nt = 4.0$, $Ld_2 = 1$, Pr = 1

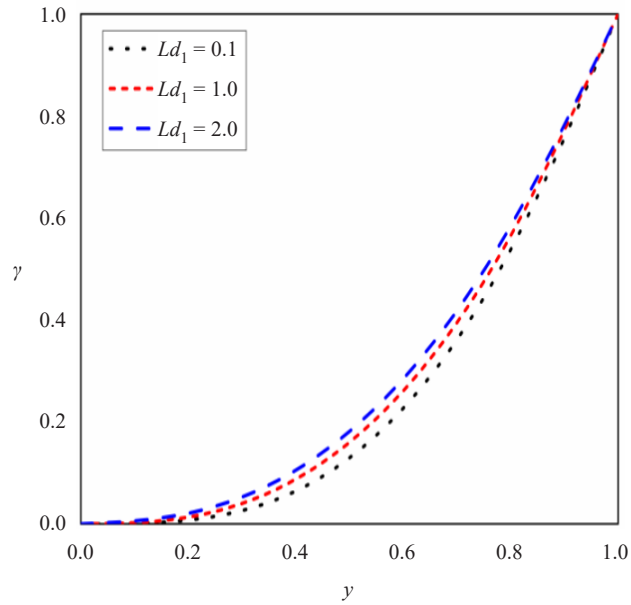

Figure 16. Variation of Ld_1 on γ
$Nb = 2.0$, $Nt = 2.0$, $Ld_2 = 2.0$, $Nd_1 = 2.0$, $Nd_2 = 2.0$, Pr = 7

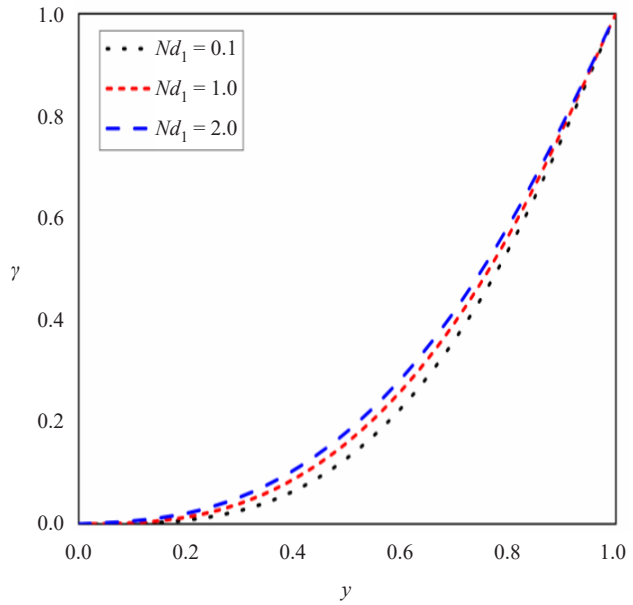

Figure 17. Variation of Nd_1 on γ
$Nb = 2.0$, $Nt = 2.0$, $Ld_1 = 2.0$, $Ld_2 = 2.0$, $Nd_2 = 2.0$, Pr = 7

4. Conclusion

This article investigates the triple diffusive convection of the peristaltic flow of Jeffrey nanofluid through a non-uniform channel. It's worth noting that the HPSTM finds the solution without using an initial guess or auxiliary linear operator, and it avoids round-off errors. This study is applicable in engineering and scientific fields like geology,

astrophysics, disposals of nuclear waste, deoxyribonucleic acid (DNA), and chemical engineering. The present work is compared with the exact solution, and it is in good agreement with the present method. The major outcomes are listed below.

- The behavior of Gr_{C_1} and Ld_1 on velocity and pressure gradient is similar.
- Similar behavior of Nb, Nt, Ld_1, Nd_1 on temperature profile.
- Similar behavior of Nb, on the concentrations of salt 1 and salt 2.
- Ld_1 and Ld_2 increase as the concentrations of salt 1 and salt 2 increase respectively.
- Jeffrey fluid parameter λ_1 and Dufour solutal Lewis number of salt 2 Ld_2 have similar behavior on velocity profile.

Conflict of interest

The authors declare that there is no personal or organizational conflict of interest with this work.

References

[1] R. W. Griffiths, "The Influence of third diffusing component upon the onset of convection," *Journal of Fluid Mechanics*, vol. 92, no. 4, pp. 659-670, 1979.

[2] R. W. Griffiths, "A note on the formation of salt-finger and diffusive interfaces in three component systems," *International Journal of Heat and Mass Transfer*, vol. 22, no. 12, pp. 1687-1693, 1979.

[3] A. R. Lopez, A. R. Louis, and A. J. Pearlstein, "Effect of rigid boundaries on the onset of convective instability in triply diffusive fluid layer," *Physics of Fluids A: Fluid Dynamics*, vol. 2, no. 6, pp. 897-902, 1966.

[4] A. J. Pearlstein, R. M. Haris, and G. Terrones, "The onset of convective instability in a triply diffusive fluid layer," *Journal of Fluid Mechanics*, vol. 202, pp. 443-465, 1989.

[5] D. Poulikakos, "The effect of third diffusing component on the onset of convection in a horizontal porous layer," *The Physics of Fluids*, vol. 28, no.10, pp. 3172-3174, 1985.

[6] N. Rudraiah, and D. Vortmeyer, "The influence of permeability and of a third diffusing component upon the onset of convection in a porous medium," *International Journal of Heat and Mass Transfer*, vol. 25, no. 4, pp. 457-464, 1982.

[7] T. W. Latham, *Fluid motion in peristaltic pump*. M.S. Thesis, Massachusetts Institute of Technology, Cambridge, MA, 1966.

[8] A. H. Shapiro, M. Y. Jaffrin, and S. L. Weinberg, "Peristaltic pumping with long wavelength at low Reynolds number," *Journal of Fluid Mechanics*, vol. 37, no. 4, pp. 799-825, 1969.

[9] M. Y. Jaffrin, and A. H. Shapiro, "Peristaltic pumping," *Annual Review of Fluid Mechanics*, vol. 3, no. 1, pp. 13-37, 1971.

[10] S. K. Asha, and G. Sunitha, "Influence of thermal radiation on peristaltic blood flow of a Jeffrey fluid with double diffusion in the presence of gold nanoparticles," *Informatics in Medicine Unlocked*, vol. 17, pp. 100272, 2019.

[11] S. K. Asha, and N. Kallolikar, "Thermal analysis for peristaltic flow of nanofluid under the influence of porous medium and double diffusion in a non-uniform channel using Sumudu transformation method," *Annals of Pure and Applied Mathematics*, vol. 23, no. 2, pp. 73-91, 2021.

[12] B. B. Gupta, and V. J. Seshadri, "Peristaltic pumping in non-uniform tubes," *Journal of Biomechanics*, vol. 9, no. 2, pp. 105-109, 1976.

[13] L. M. Srivastava, V. P. Srivastava, and S. N. Sinha, "Peristaltic transport of a physio-logical fluid," *Biorheology*, vol. 20, no. 2, pp. 153-166, 1983.

[14] S. K. Asha, and G. Sunitha, "Peristaltic transport of Eyring-Powell nanofluid in a non-uniform channel," *Jordan Journal of Mathematics and Statistics*, vol. 12, no. 3, pp. 431-453, 2019.

[15] S. K. Asha, and G. Sunitha, "Effect of joule heating and MHD on peristaltic blood flow of Eyring-Powell nanofluid in a non-uniform channel," *Journal of Taibah University for Science*, vol. 13, no. 1, pp. 155-168, 2019.

[16] K. K. Raju, and R. Devanathan, "Peristaltic motion of a non-Newtonian fluid," *Rheological Acta*, vol. 11, no. 2, pp. 170-178, 1972.

[17] K. L. Jyothi, P. Devaki, and S. Sreenadh, "Pulsatile flow of a Jeffrey fluid in a circular tube having internal porous

lining," *International Journal of Mathematical Archive*, vol. 4, no. 5, pp. 75-82, 2013.
[18] N. S. Akbar, S. Nadeem, and C. Lee, "Characteristics of Jeffrey fluid model for peristaltic flow of chyme in small intestine with magnetic field," *Results in Physics*, vol. 3, pp. 152-160, 2013.
[19] H. Eltayeb, and A. Kilicman, "A note on the Sumudu transforms and differential equations," *Applied Mathematical Sciences*, vol. 4, no. 22, pp. 1089-1098, 2010.
[20] F. B. M. Belgacem, A. A. Karaballi, and L. S. Kalla, "Analytical investigations of the sumudu transform and applications to integral production equations," *Mathematical Problems in Engineering*, vol. 3, pp. 103-118, 2003.
[21] G. K. Watugala, "Sumudu transform-A new integral transform to solve differential equations and control engineering problems," *Integrated Education*, vol. 24, no. 1, pp. 35-43, 1993.